Surface & Coatings Technology 313 (2017) 184–190

Contents lists available at ScienceDirect

Surface & Coatings Technology

journal homepage: www.elsevier.com/locate/surfcoat

A finite element assessment of influential factors in evaluating interfacial fracture toughness of thermal barrier coating

Yoshifumi Okajima [a,*], Motoki Sakaguchi [b], Hirotsugu Inoue [b]

[a] Research and Innovation Center, Mitsubishi Heavy Industries, Ltd., 2-1-1 Shinhama, Arai-cho, Takasago, Hyogo 676-8686, Japan
[b] Department of Mechanical Engineering, Tokyo Institute of Technology, 2-12-1 Ookayama, Meguro-ku, Tokyo 152-8552, Japan

ARTICLE INFO

Article history:
Received 27 September 2016
Revised 12 December 2016
Accepted in revised form 16 January 2017
Available online 17 January 2017

Keywords:
Interfacial fracture toughness
Circumferential crack
Tensile test
Thermal barrier coating
Residual stress
Finite element analysis

ABSTRACT

It was previously reported that the adhesion strength of thermal sprayed yttria-stabilized zirconia coatings, as measured by the modified tensile test, decreased with increased coating thickness. Results from this method include the effects of both residual stress introduced during the spraying process and the adhesive glue used for the specimen preparation. This work quantified these effects by means of finite element analysis. The model also considered friction factors for interfacial crack closure induced by compressive residual stress in the coatings. It is concluded that friction factors affect interfacial fracture toughness slightly, but the most significant effect is caused by a change in the crack propagation path in the case of the thinnest coatings.

1. Introduction

From the so-called 3E viewpoint, which represents economic efficiency, the environment, and energy security, all countries are encouraged to make better use of fossil fuels. Gas turbine combined cycle (GTCC) technology is therefore starting to play a more significant role in power generation systems because of its high thermal efficiency. Demands for GTCC efficiency to be even higher have led to increasing gas turbine inlet temperatures. The most advanced gas turbine, which achieves a temperature of about 1600 °C, employs a thermal barrier coating (TBC) that is essential to protect the blade and vanes from such a hot gas stream [1]. Any spalling of the TBC can cause catastrophic damage to the turbine. Evaluation of adhesion strength of the coating is therefore required for all fields of application. One of the most promising evaluation methods is based on interfacial fracture mechanics [2–4]; however, problems relating to interfacial mechanics always involve difficulties, including those of mixed-mode stress fields and stress–strain singularity. Residual stress induced by the coating process also has significant effects on the adhesive strength [5–7].

Various testing methods [8–12] have been developed to evaluate interfacial fracture toughness; however, most procedures and sample preparations are cumbersome. Some are limited in applicability to ductile materials or adhesive polymers [8,9]; others require complicated equipment [10,11]. Although an indentation test [12] is simple, it includes some error in measurement of crack length, depending on the skill and experience of the observer. The modified tensile test proposed by Watanabe et al. [13] is one of the simplest methods, and it can be conducted using only a tensile testing system and can be applied to brittle ceramic coatings [14].

In a previous study, the authors used this modified tensile test to evaluate a TBC applied by thermal spraying, and reported that its adhesion strength decreased with coating thickness, as shown in Fig. 1 [15]. It was, however, not clear why a thicker coating showed lower adhesion strength. Possible reasons are: (i) changes of the stress field due to variations of coating thickness and Young's modulus; (ii) a contribution from residual stress within the coatings induced by the spraying process; (iii) an effect of the adhesive layer used during sample preparation. It is difficult to experimentally evaluate each factor individually because they mutually interact and complicate the phenomenon.

In this work, effects of experimental variables on the interfacial fracture toughness, as measured by the modified tensile test, were numerically evaluated to investigate reasons why a thicker coating showed lower adhesion strength. Energy release rate was calculated using a finite element model (FEM) that simulated actual geometry and measured coating modulus of a test specimen. Residual stress accumulated during the spraying process was simulated by thermal mismatch between the coating and substrate; influence of crack–surface contact was also considered. Adhesive glue was also modeled to confirm how this can affect test results.

* Corresponding author.
E-mail address: yoshifumi_okajima@mhi.co.jp (Y. Okajima).

http://dx.doi.org/10.1016/j.surfcoat.2017.01.052
0257-8972/

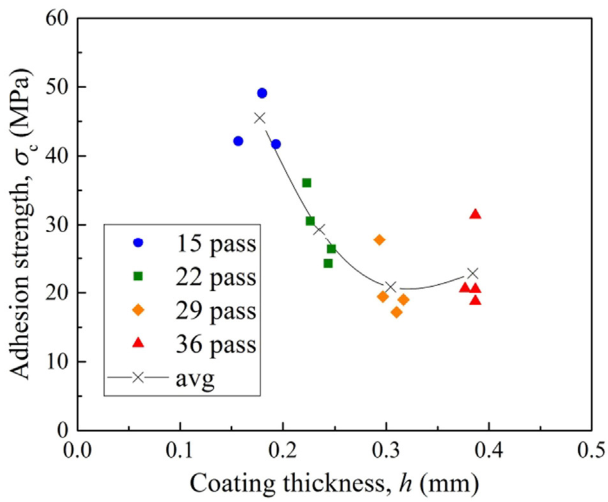

Fig. 1. Adhesive strength results for various thicknesses of thermal barrier coating, as measured by the modified tensile test [15].

2. Analysis of modified tensile test

2.1. Previous study and its problems

In the modified tensile test, a coating is processed on a cylindrical substrate with a circumferential pre-crack around its outer edge. Another cylinder is then bonded to the coating surface using adhesive glue. Adhesion strength between the coating and substrate can be evaluated by measuring the tensile load when the coating is de-bonded from the substrate. Watanabe et al. [13] analyzed the modified tensile test using FEM and formulated interfacial stress intensity factors, F_i, normalized by $\sigma_\infty\sqrt{\pi a}$ as:

$$F_i = (1-\alpha)^{1/2}\left(\frac{c}{R}\right)^{-3/2}\cdot G\left(\frac{c}{R}\right), \tag{1}$$

where σ_∞ is nominal stress, R is the substrate radius, a is crack length, $c(=R-a)$ is ligament length, α is the Dundurs parameter, defined in [16], and $G(c/R)$ is a shape factor, as defined in Eq. (2):

$$G\left(\frac{c}{R}\right) = \frac{1}{2}\left\{1+\frac{1}{2}\left(\frac{c}{R}\right)+\frac{3}{8}\left(\frac{c}{R}\right)^2-0.363\left(\frac{c}{R}\right)^3+0.731\left(\frac{c}{R}\right)^4\right\}. \tag{2}$$

Using Eq. (1), the stress intensity factor for a homogeneous material with a circumferential crack was extended [17] to a bi-material crack, based on the analysis of a sandwich structure [18]. Eq. (1) is accurate enough to obtain interfacial stress intensity factors for engineering applications, but it provides no quantitative information concerning the effects of various factors, including those of coating thickness and residual stress in the coating.

2.2. Description of finite element model

Fig. 2 shows the two-dimensional (2D) FEM configurations employed in this study. Complex stress intensity factors in the modified tensile test specimen were analyzed using whole specimen models, as shown in Fig. 2(a) and (b). The commercial code *ABAQUS 6.13* (Simulia, Providence, RI, USA) was used. The model in Fig. 2(b) includes an adhesive layer between the coating and the Al substrate. Stress intensity factors caused by residual stress were independently calculated using an as-sprayed model, shown in Fig. 2(c). Because the crack-tip stress field caused by residual stress is independent of that induced by a tensile applied load, the stress intensity factors from residual stress can be superposed on that calculated for the whole specimen model, as in Fig. 2(a) or (b).

Fig. 3 shows detailed FEM meshes for three cases. In all models, eight-node quadratic elements with axis symmetry were used. The bottom surfaces of the Al substrates were restrained in the vertical direction. An adhesive layer composed of eight meshes was inserted between the coating and top substrate. A fine mesh was generated from the crack tip in the radial direction and quarter-point singular elements were employed around the crack tip, the size of which was 1 μm in length. Complex stress intensity factors and *J*-integrals (energy release rates) were computed using the interaction integral method [19]. Analyses were attempted for various combinations of moduli and

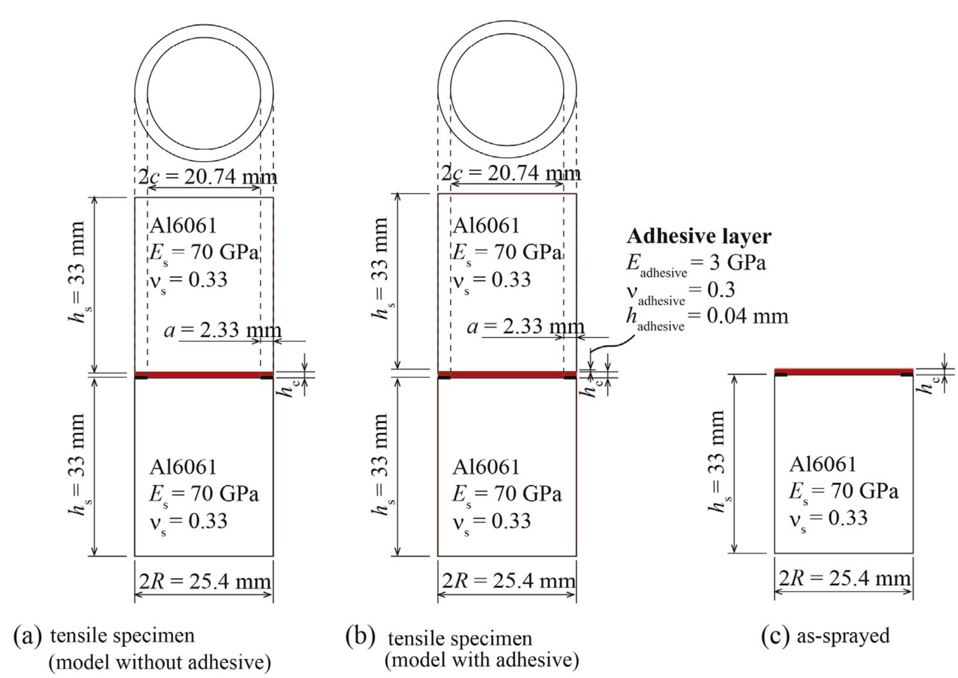

Fig. 2. Finite element model configurations and materials properties.